Cool Methane Oxidation

DOI: 10.1002/anie.201108706

Direct Catalytic Conversion of Methane to Methanol in an Aqueous Medium by using Copper-Promoted Fe-ZSM-5**

*Ceri Hammond, Michael M. Forde, Mohd Hasbi Ab Rahim, Adam Thetford, Qian He, Robert L. Jenkins, Nikolaos Dimitratos, Jose A. Lopez-Sanchez, Nicholas F. Dummer, Damien M. Murphy, Albert F. Carley, Stuart H. Taylor, David J. Willock, Eric E. Stangland, Joo Kang, Henk Hagen, Christopher J. Kiely, and Graham J. Hutchings**

The selective oxidation of primary carbon–hydrogen bonds is of crucial importance in activating raw materials to form intermediates and final products for use in the chemical, pharmaceutical, and agricultural business sectors. One of the most challenging reactions of this type is the oxidation of methane to methanol. Methanol is currently produced from methane in an energy-intensive two-stage process through the intermediate manufacture of synthesis gas,[1] though a one-step selective oxidation would present both economic and environmental advantages. In nature, methane monooxygenase (MMO) demonstrates that a one-step oxidation is feasible under mild aqueous conditions, but delivery of oxygen involves complex co-enzymes and rates that are not commercially viable.[2] To date viable chemical catalytic routes have proven elusive. Approaches using oxide or metal catalysts at high temperature, typically $>600\,^{\circ}C$, achieve only limited methanol selectivity.[3,4]

Low temperature approaches on the other hand usually require multiple steps and so do not give a closed catalytic cycle, or they proceed at low catalytic rates (turnover frequencies $<10\,h^{-1}$).[5–16] Of particular interest are the studies involving iron (copper) zeolites that when activated with N_2O (oxygen) at high temperature can react with methane to form surface methoxy species which later require hydrolysis at a lower temperature to form methanol,[8,14–17] and we therefore used this as the starting point for our low temperature methane oxidation studies. We reasoned that it should be feasible to access an active oxygen species using aqueous hydrogen peroxide, which would also act for hydrolysis of intermediates and thereby construct a closed catalytic cycle. Here we show that iron- and copper-containing zeolites catalyze the oxidation of methane to methanol in aqueous conditions using hydrogen peroxide.

We discovered that, following high-temperature calcination, commercial ZSM-5 displays significant catalytic activity for the selective oxidation of methane using aqueous conditions at low temperatures (Table 1, entry 1). This activity depends on both the SiO_2/Al_2O_3 ratio and the activation procedure, with a heat pre-treatment at 550 °C for 3 h giving both high oxygenate productivity and selectivity to partial oxidation products. The level of activity exhibited by ZSM-5 has so far proven to be unique; other zeolites with similar compositions, but different pore structures, are an order of magnitude less active (Supporting Information, Table S1). We initially found that a molecular confinement effect within the zeolite micropores alone was unable to induce catalytic activity, as silicalite-1 was found to be inactive (Table 1, entry 2). A significant difference between silicalite-1 and ZSM-5 is the aluminium content and we therefore tuned the composition of the zeolite to identify the source of activity. We discovered that varying the aluminium content of ZSM-5 (30), through post-synthesis or hydrothermal methods (metal, M, introduced post-synthesis is denoted as M/ZSM-5; metals incorporated through the synthesis gel are denoted as M-ZSM-5), led to negligible changes in activity (Table 1, entry 3, Figure S1). We therefore concluded that Al was not the active component of the catalyst.

In view of these results, elemental analysis of the commercial materials was performed in order to determine the role played by any potential impurity metal species within the structure. This analysis revealed that each sample contained trace amounts of the transition metals Fe and Ti (Table S2) that are known to activate hydrogen peroxide.[13,18] TS-1 was found to be inactive, but introducing Fe alone into the inactive silicalite-1 matrix by hydrothermal synthesis leads to a significant increase in activity, strongly suggesting that Fe species are the active component of the catalyst (Figure S1). Fe-silicalite-1 also proved to be a highly active and re-usable heterogeneous catalyst (Table S3), and under

[*] Dr. C. Hammond, M. M. Forde, Dr. M. H. Ab Rahim, A. Thetford, Dr. R. L. Jenkins, Dr. N. Dimitratos, Dr. J. A. Lopez-Sanchez, Dr. N. F. Dummer, Dr. D. M. Murphy, Dr. A. F. Carley, Dr. S. H. Taylor, Dr. D. J. Willock, Prof. G. J. Hutchings
Cardiff Catalysis Institute, School of Chemistry, Cardiff University
Main Building, Park Place, Cardiff, CF10 3AT (UK)
E-mail: hutch@cardiff.ac.uk

Q. He, Prof. C. J. Kiely
Center for Advanced Materials and Nanotechnology
Lehigh University, Bethlehem, PA 18015-3195 (USA)

Dr. E. E. Stangland, Dr. J. Kang
National Corporate R&D, The Dow Chemical Company
Midland, MI 48674 (USA)

Dr. H. Hagen
Dow Benelux B. V., Herbert H. Dowweg 5, 4542 NM HOEK
Postbus 48, 4530 AA Terneuzen (The Netherlands)

[**] This work formed part of the Methane Challenge. The Dow Chemical Company is thanked for their financial support. Computing facilities for this work were provided by ARCCA at Cardiff University, HPC Wales, and through our membership of the UK's HPC Materials Chemistry Consortium (MCC). The MCC is funded by EPSRC (EP/F067496).

Supporting information for this article is available on the WWW under http://dx.doi.org/10.1002/anie.201108706.

Table 1: Catalytic studies of Fe-containing zeolites for the oxidation of methane under mild conditions.[a]

Entry	Catalyst	Fe content [wt.%]	Preparation procedure	Initial methane [mmol]	Product amount [μmol]				Oxy. sel. [%][d]	CH_3OH sel. [%][e]	Conv. [%][f]
					MeOH[b]	HCOOH[b]	MeOOH[b]	CO_2 (g)[c]			
1	ZSM-5 (30)	0.014	commercial	30.8	15.4	44.0	17.7	4.4	95	19	0.3
2	silicalite-1	0	hydrothermal	30.8	0.0	0.0	0.0	0.0	–	–	tr.
3	Al/ZSM-5 (30)	0.014	SSIE	30.8	15.8	40.4	15.3	1.5	98	22	0.2
4	TS-1	–	commercial	30.8	0.2	0.0	1.0	0.1	99	15	0.0
5	Fe/ZSM-5 (30)	2.5	SSIE	30.8	22.3	164.0	1.8	38.6	83	12	0.7
6	Fe-silicalite-1	0.5	hydrothermal	30.8	15.4	60.5	7.5	5.8	94	17	0.3
7	$Fe(NO_3)_3$	23	commercial (10 μmol Fe)	30.8	3.5	10.4	5.8	18.9	51	9	0.1
8	ZSM-5 (30)/Na_2SO_3	0.014	commercial	30.8	22.9	29.4	17.5	2.1	97	32	0.2
9	$Fe(NO_3)_3/Na_2SO_3$	23	(10 μmol Fe)	30.8	1.3	1.6	4.5	1.3	85	15	tr.
10	Cu/ZSM-5 (30)	0.014	SSIE	30.8	65.3	0.0	6.2	6.9	88	83	0.3
11	Cu-Fe/ZSM-5 (30)	2.5	SSIE	30.8	188.8	0.0	0.5	33.3	85	85	0.7
12	Fe/ZSM-5 (30)/$Cu(NO_3)_3$ (aq)	2.5	SSIE (10 μmol Cu)	30.8	140.1	0.0	1.1	18.8	88	88	0.5
13	Cu/silicalite-1	0	SSIE	30.8	0.0	0.0	0.0	0.0	–	–	0.0
14	Fe-silicalite-1[g]	0.5	hydrothermal	1.8	15.1	156.7	10.2	7.6	96	8	10.5
15	Fe-silicalite-1 and Cu/silicalite-1[g]	0.5	hydrothermal SSIE	1.8	168.4	0	0	12.5	93	93	10.1

[a] Standard reaction conditions: 10 mL, 30 min, 50 °C, $P_{(CH4)}$ 30.5 bar, [H_2O_2] 0.5 M, catalyst 27 mg, 1500 rpm. Typical catalyst pre-treatment: calcination (550 °C, 3 h, static air). SSIE corresponds to samples prepared by solid state ion-exchange. [b] Analyzed by ^{1}H NMR with 1% tetramethylsilane (TMS) in $CDCl_3$ internal standard. [c] Analyzed by GC-FID. [d] Oxygenate selectivity, calculated as moles (oxygenates)/moles (produced) × 100. [e] Methanol selectivity, calculated as moles (MeOH)/moles (produced) × 100, [f] Conversion, calculated as (moles produced)/(initial moles methane) × 100, tr. represents trace (i.e. < 0.01%). [g] Reaction conditions standard except: 20 mL, 70 °C, $P_{(CH4)}$ 3 bar, [H_2O_2] 1.0 M, catalyst 54 mg.

appropriate reaction conditions a 10% conversion with 96% selectivity to partially oxygenated products (CH_3OH, CH_3OOH, HCOOH) was achieved (Table 1, entry 14). These experiments demonstrate that the presence of Fe within the MFI material is crucial for significant catalytic activity, and that concentrations as low as 120 ppm (as found in commercial ZSM-5 samples) are sufficient for the formation of highly active catalysts (Table S2).[19–21] In addition, experiments using ^{1}H NMR spectroscopy of the reaction mixture using ^{13}C labeled methane confirms that the oxygenate products observed are derived from the CH_4 reactant (Figure S2).

In view of the linear relationship between Fe content and activity, and its controlled synthesis procedure and lack of impurities, we systematically investigated the nature of the Fe species within Fe-silicalite-1 in order to determine a link between catalyst structure and activity. Transmission electron microscopy (TEM)/X-ray energy dispersive spectroscopy (XEDS) and X-ray photoelectron spectroscopy (XPS) both confirmed the absence of Fe species on the external surface of the catalyst (Figure S3 and S4). We therefore focused on the nature of the active Fe species within the zeolite micropores with FT-IR and UV/Vis spectroscopy. In the as-prepared Fe-silicalite-1 material, FT-IR spectra showed a band at 710–700 cm^{-1} indicative of Fe incorporation into tetrahedral framework sites (Figure S5).[22] However, following template removal and calcination (required for high activity) this band is significantly diminished, suggesting migration of the Fe ions from the framework to extra-framework positions. UV/Vis studies also confirmed the migration of Fe ions upon heat pre-treatment, and demonstrated that increased activity correlates with an increasing extra-framework component (Figure S6). Analogous analysis of commercial ZSM-5 (30) by X-ray absorption near edge structure (XANES) measurements also demonstrated that within this sample, an increased octahedral (extra-framework) component was observed upon heat pre-treatment (Figure S7). The extraction of Fe from the zeolite framework following thermal pre-treatment is in line with previous studies of (activated) Fe-containing zeolites.[23–25] In summary, an increased concentration of octahedral (extra-framework) Fe is accompanied by significant increases in catalytic activity.

The specific geometrical environment of the extra-framework Fe species was thus investigated by EXAFS, which showed that the Fe–Fe coordination number was low (1.6), with an average Fe–Fe distance of 2.97 ± 0.04 Å, and an average Fe–O separation of 2.04 ± 0.02 Å (Table S4). We note that these values are consistent with previously reported diiron species within zeolites.[26–28] Based on these experimental findings, periodic DFT calculations were used to simulate model extra-framework diiron species in an MFI-framework with two counter-cation exchange sites.[9] Several alternative model structures were evaluated and optimized (Figure S8, Table S5), and the closest match between EXAFS experiment and theoretical modeling was obtained for a diiron complex $[Fe_2(\mu_2\text{-}OH)_2(OH)_2(H_2O)_2]^{2+}$, containing antiferromagnetically coupled high-spin octahedral Fe^{3+} centers. We thus use this model to represent the resting state of the active site in ZSM-5 (**1**, Figure 1C).

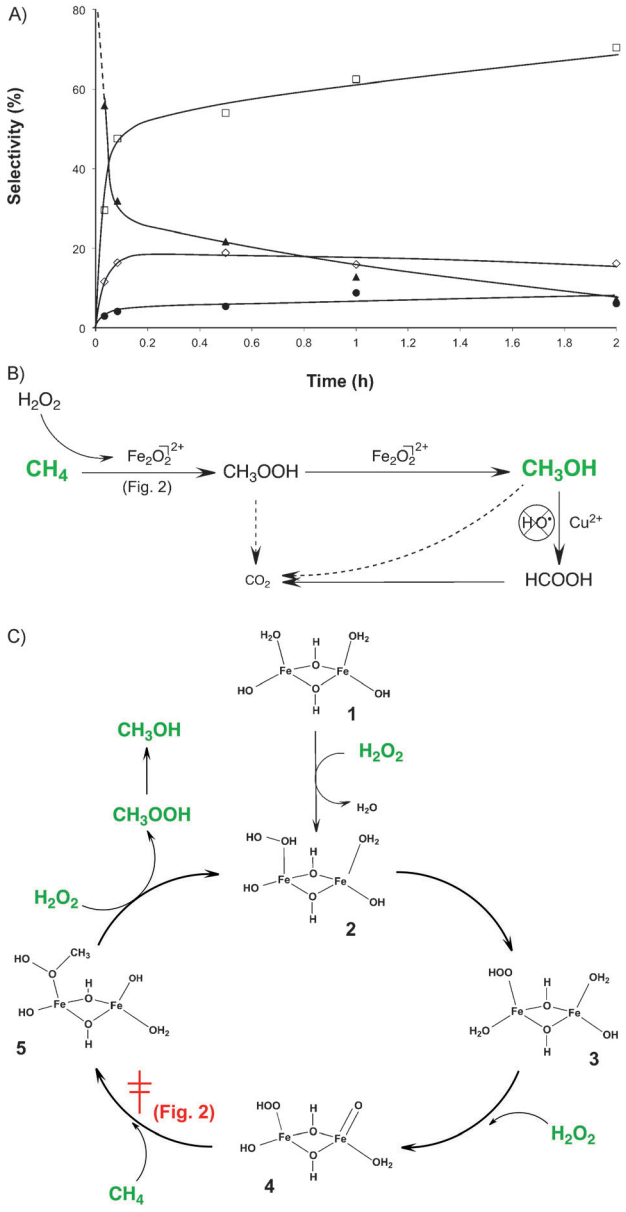

Figure 1. A) Time-on-line profile for the liquid-phase oxidation of methane with hydrogen peroxide and ZSM-5 (30). Key: ▲ = methyl hydroperoxide (MeOOH); ◇ = methanol (MeOH); □ = formic acid (HCOOH); ● = carbon dioxide (CO_2). B) A potential reaction scheme for the oxidation of methane based on the time-on-line profile. Methanol is formed through the conversion of the methyl hydroperoxide intermediate over the Fe sites present in the catalyst. •OH radicals produced during the reaction are later responsible for the over-oxidation of methanol. C) Catalytic cycle for the oxidation of methane to CH_3OOH using H_2O_2, catalyzed by a binuclear Fe species in ZSM-5. The overall charge in each case is formally +2 as the species acts as an extra-framework cation within the zeolite.

Starting from this resting state, the DFT calculations were extended to build a molecular level mechanism for methane oxidation that is consistent with the experimental data. Time-on-line analysis has revealed that methyl hydroperoxide (CH_3OOH) is the primary reaction product (Figure 1 A), and that methanol, formic acid, and CO_2 are formed consecutively (Figure 1 B). Within this proposed cycle, the diiron site, **1**, first coordinates H_2O_2 through exchange with a water ligand to give species **2**. H^+-transfer and solvent rearrangement then gives **3** which is formally an Fe^{4+}/Fe^{2+} dimer, although DFT optimization offsets the μ_2-OH ligands toward Fe^{2+} (average Fe–(μ_2-OH) 2.06(Fe^{4+}) cf. 1.91(Fe^{2+})). A second H_2O/H_2O_2 exchange places H_2O_2 at the Fe^{2+} site, although this cannot give a second surface hydroperoxide because there is no adjacent ligand that can easily abstract H^+. However, Fe^{2+}(aq) has been shown to react with H_2O_2 to produce a ferryl ion (Fe^{4+}=O) in Fenton's reagent,[29,30] and we propose a similar event here to generate **4**. In contrast to a Fenton's or an α-oxygen-type mechanism, which proceed through isolated Fe^{4+}=O sites, the formation of an Fe^{4+}=O species adjacent to Fe–OOH results in a novel, bifunctional oxidation center, **4**, and this has a profound effect on the methane activation process. Starting from species **4**, the reaction pathway from an adsorbed methane molecule (Figure 2,

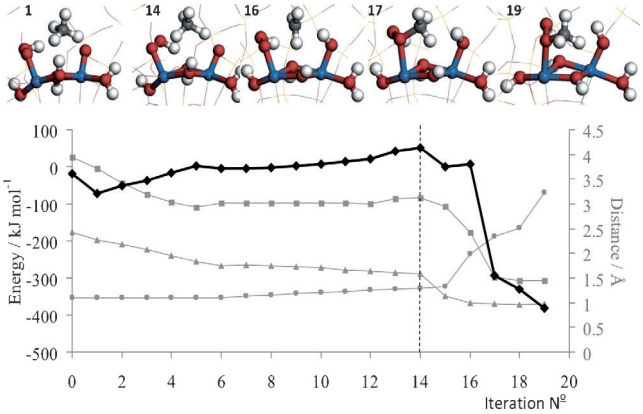

Figure 2. Spin-unrestricted DFT-optimized (PBE, U_{Fe} = 4.0) pathway for methane to methyl hydroperoxide showing energy relative to the free methane, hydroperoxide and resting state of the catalyst (in black referred to left-hand axis, diamonds) and (in gray referred to the right-hand axis) the key atom distances along the pathway, with H_3C···OOH as triangles, (H$_3$C)H···O=Fe as squares and H_3C···H as diamonds. The *x*-axis is the iteration number along the reaction coordinate. Top: graphical representations of the active-site region at the points along the reaction coordinate indicated by iteration number are given, in each case the reactants and molecules coordinated to Fe centers are shown in ball-and-stick representations while the zeolite framework is wireframe, most of the periodic structure of the MFI unit cell is omitted for clarity. Atoms colored according to C gray, O red, H white, Si yellow(wire), Al pink(wire), Fe mauve. Further details of method are deposited in the Supporting Information.

iteration 1) to the adsorbed product (methyl hydroperoxide) (Figure 2, iteration 19) was mapped out using periodic DFT. Initially the Fe^{4+}=O iron atom has a high spin state due to the relatively weak field ligands surrounding this ion, which makes the oxo group reactive for the abstraction of H from methane.[31] In the reaction profile the C–H bond length gradually increases, until at C–H = 1.30 Å H transfer to the oxo group occurs (Figure 2, iteration 14). Whilst a methyl radical is indicated after the top of the barrier (Figure 2, iteration 16), this is a transient intermediate species that is immediately captured by the hydroperoxy ligand at the

second Fe center, thus forming the $(H_3)C{-}OOH$ bond and not releasing free methyl radicals (Figure 2, iteration 17).

To confirm the validity of this model, we experimentally investigated the potential radical species formed during the reaction through additional spectroscopic techniques (Table S6). Although the oxidising ability of these catalysts prevents the testing of the mechanism through radical clock chemistry,[32] the system is amenable to study with EPR spectroscopy (with 5,5-dimethylpyrroline-*N*-oxide (DMPO)) and radical scavengers. The absence of methyl radical signals in the EPR spectra is in agreement with the molecular mechanism proposed above. Furthermore, the absence of methyl radicals distinguishes the chemistry reported here from previous studies of methane activation by either α-oxygen, derived from N_2O[7–9] or Fenton's reagent;[13,29] in these systems, methyl radicals have been observed and implicated as essential features of the corresponding mechanisms. We consider the new mechanism to be of paramount importance to the high oxygenate selectivities we observe, as systems operating through methyl free radical chemistry with terminal oxidants (cf. Fenton's chemistry) typically show low oxygenate selectivity, (e.g. Table 1, entry 8). After formation of the primary product (methyl hydroperoxide), the active site (Figure 1 C, **2**) is regenerated by the desorption of methyl hydroperoxide into solution, thereby closing the catalytic cycle. Our proposed mechanism implies a stoichiometry of 2:1 (H_2O_2:CH_4), which is the lowest ratio we have observed experimentally with calcined ZSM-5 (30) (Table S7). Additionally, we found that the DFT-calculated barrier for this new oxidation pathway was 50 kJ mol^{-1} relative to the free reagents and catalyst (Figure 2), which is lower than estimates for MMO,[33,34] and in good agreement to the experimentally determined activation energy of 61 kJ mol^{-1} (Figure S9). Although the mechanism is consistent with all available experimental data to hand, in subsequent studies we aim to carry out spectroscopic investigations to test the proposed mechanism in more detail.

To account for the observation of consecutive oxidation products (Figure 1 A), we considered that methyl hydroperoxide may subsequently undergo a second surface catalyzed conversion to methanol through the hydrolysis of a surface-bound methoxy species (Figure S10). This process will generate hydroxyl radicals, which we propose to facilitate the over-oxidation of methanol to formic acid. EPR radical trapping studies later confirmed that, whilst carbon-centered radicals were not detected, significant quantities of ·OH radicals were produced during the reaction (Figure S11). These presumably arose from the non-selective decomposition of hydrogen peroxide or the alkyl hydroperoxy RO–OH bond during the catalytic cycle. To investigate the role of these species, an ·OH radical scavenger (Na_2SO_3) was used. Whilst no change in reaction rate was observed with Na_2SO_3, methanol selectivity increased from 19% to 32%, demonstrating that ·OH radicals are involved in the over-oxidation of methanol (Table 1, entry 11, Figure S12). The presence of ·OH radicals and their role in methanol over-oxidation could be a major limitation since methanol is the target product.

We therefore focused our studies on improving the selectivity to methanol. During these studies, we identified that the addition of Cu^{2+} to the reaction, either as a component of the heterogeneous catalyst, or as a heterogeneous or homogeneous additive to the reaction mixture drastically reduces the over-oxidation process, and yields methanol as the major reaction product at selectivities above 85% (Table 1, entries 10–13, Figure S13). Despite this, Cu^{2+} is not responsible for methane activation as no increase in catalyst productivity was observed after its addition to the catalyst, or the reaction solution (Table 1, entries 10–13). To understand the positive role of Cu^{2+}, further investigations with EPR spectroscopy were carried out which revealed that in reactions catalyzed by Cu-containing ZSM-5, hydroxyl radicals were no longer observed (Figure S14). These results clearly indicate that the increase in methanol selectivity is due to a decrease in concentration of hydroxyl radicals, as found when using Na_2SO_3 as a radical scavenger. By combining the effect of Cu with the high activity of Fe, we found that a physical mixture of Cu/silicalite-1 and Fe-silicalite-1 to be sufficient to produce a highly selective catalytic system that achieved a methane conversion of 10% with 93% selectivity to methanol (Table 1, entry 15).

Given that the catalytic data and spectroscopic analysis has identified Fe as the key catalytic component in the oxidation of methane, this allows normalized turnover frequencies (TOF: mol(product) mol^{-1}(metal) h^{-1}) and volume productivities (moles liquid phase oxygenates cm^{-3} s^{-1}) to be calculated and compared with other methane oxidation approaches (Table 2 and S8). We observe TOFs $>2200\ h^{-1}$ under standard conditions (Table 2, entry 2), which increase to $>14000\ h^{-1}$ at initial reaction periods (2 min) (Table 2, entry 3). These TOF values are up to three orders of magnitude greater than any chemical system previously reported, and in the presence of Cu, these TOFs are retained at a methanol selectivity >90%. We also note that, in contrast to the previous zeolite-based approaches, this Fe- and Cu-based system operates through a closed catalytic cycle, permitting high methane conversions and high oxygenate selectivity to be obtained.

The general applicability of the batch reaction process has also been probed with ethane, for which a conversion of 56% with partial oxygenate selectivity of 97% was obtained under optimized conditions (Table S9), showing that this oxidation system may also find future applications for the partial oxidation of higher alkanes.

In summary, we show that iron- and copper-containing zeolites catalyze the oxidation of methane to methanol in aqueous conditions using hydrogen peroxide, with activities that are three orders of magnitude higher than any previously reported. Through a combination of catalytic, spectroscopic, and computational investigations, we demonstrate that the interaction between Fe-ZSM-5 and hydrogen peroxide results in a low-energy pathway for methane oxidation, which is distinguished from Fenton's chemistry, α-oxygen, and an MMO-type rebound mechanism. Hydrogen peroxide reacts at the iron centers to produce species capable of the activation of the carbon–hydrogen bond, forming methyl hydroperoxide as the primary product. Whilst copper does not play a direct role in methane activation, it facilitates the formation of methanol by inhibiting over oxidation to formic acid and CO_2.

Table 2: Comparison of methane oxidation catalysts.

	Catalyst	CH_3OH sel. [%][a]	TOF [h^{-1}][b]	Volume prod.[c]	Catalytic cycle? (TON)	Ref.[d]
1	sMMO	100	95	2.8×10^{-9}	yes (19)	[2]
2	ZSM-5 (30)	18	2278	4.3×10^{-9}	yes (>1139)	this work
3	ZSM-5 (30)	12	6320	1.2×10^{-8}	yes (>3000)	this work
4	Cu/ZSM-5 (30)	83	2113	4.0×10^{-9}	yes (>1057)	this work
5	Fe-silicalite-1 and Cu/silicalite-1	93	70	4.7×10^{-9}	yes (>35)	this work
6	Fe-ZSM-5, N_2O	100	–	–	no (0.25)	[14]
7	Cu-ZSM-5	98	–	–	no (0.02)	[16]
8	(bpym)$PtCl_2$/oleum[d]	81[e]	36	2.3×10^{-7}	no[g] (>500)	[5]
9	Pt-CTF[g]	>75	98	2.0×10^{-7}	no 246	[6]
10	$FeCl_3$ (aqueous)	7	7	1.9×10^{-9}	yes (7)	[13]
11	$OsCl_3$ (aqueous)	30	12	3.3×10^{-9}	yes (30)	[13]
12	$FeCl_{16}$Pc-Na-X[h]	53	9	2.9×10^{-10}	yes (107)	[10]
13	$(Fe^t BuPc)_2N/SiO_2$[i]	0	6	1.5×10^{-9}	yes (209)	[11]

[a] Moles (MeOH)/moles (produced)×100. [b] Moles (products)/(mole (metal)×reaction time). [c] Moles (liquid phase oxygenates)/(reaction volume×reaction time) [d] (bpym)$PtCl_2$ = dichloro(η-2-{2,2′-bipyrimidyl})platinum(II). [e] Taken from quoted yield of CH_3OSO_3H assuming complete hydrolysis. [f] TON quoted for CH_3OSO_3H rather than methanol. [g] CTF = covalent triazine-based framework, as for entry 7 primary product is CH_3OSO_3H which is hydrolyzed in a second reaction step. [h] $FeCl_{16}$Pc-Na-X = $FeCl_{16}$Pc (Pc = phthalocyanine) complex encapsulated in Na-zeolite-X. [i] $(Fe^t BuPc)_2N$ = nitrido-bis[tetra(*tert*-butyl)phthalocyaninato-iron].

While the use of hydrogen peroxide as a terminal oxidant is too expensive for use commercially with methane, we propose that the new chemistry identified will aid future catalyst design approaches for the selective oxidation of C–H bonds. It should also be noted that hydrogen peroxide may be a viable oxidant with higher hydrocarbons, and the preliminary results we show for ethane indicate that the catalyst may have applicability in such reactions.

Received: December 10, 2011
Revised: February 2, 2012
Published online: April 5, 2012

Keywords: copper · heterogeneous catalysts · iron · methane · zeolite

[1] M. V. Twigg, G. W. Bridger, M. S. Spencer, *Catalyst Handbook*, 2nd ed., Wolfe, London, **1989**.
[2] J. Colby, D. I. Stirling, H. Dalton, *Biochem. J.* **1977**, *165*, 395–402.
[3] G. J. Hutchings, M. S. Scurrell, J. R. Woodhouse, *Chem. Soc. Rev.* **1989**, *18*, 251–283.
[4] J. S. J. Hargreaves, G. J. Hutchings, R. W. Joyner, *Nature* **1990**, *348*, 428–429.
[5] R. A. Periana, D. J. Taube, S. Gamble, H. Taube, T. Satoh, H. Fujii, *Science* **1998**, *280*, 560–564.
[6] R. Palkovits M. Antonietti, P Kuhn, A. Thomas, F. Schüth, *Angew. Chem.* **2009**, *121*, 7042–7045; *Angew. Chem. Int. Ed.* **2009**, *48*, 6909–6912.
[7] N. S. Ovanesyan, A. A. Shteinman, K. A. Dubkov, V. I. Sobolev, G. I. Panov, *Kinet. Catal.* **1998**, *39*, 792–797.
[8] B. R . Wood, J. A. Reimer, A. T. Bell, M. T. Janicke, K. C. Ott, *J. Catal.* **2004**, *225*, 300–306.
[9] P. P. Knops-Gerrits, W. A. Goddard III, *J. Mol. Catal. A* **2001**, *166*, 135–145.
[10] R. Raja, P. Ratnasamy, *Appl. Catal. A* **1997**, *158*, L7–L15.
[11] A. B. Sorokin, E. V. Kudrik, L. X. Alvarez, P. Afanasiev, J. M. M. Millet, D. Bouchu, *Catal. Today* **2010**, *157*, 149–154.
[12] M. Lin, A. Sen, *Nature* **1994**, *368*, 613–615.
[13] Q. Yuan, W. Deng, Q. Zhang, Y. Wang, *Adv. Synth. Catal.* **2007**, *349*, 1199–1209.
[14] K. A. Dubkov, V. I. Sobolev, E. P. Talsi, M. A. Rodkin, N. H. Watkins, A. A. Sheinman, G. I. Panov, *J. Mol. Catal. A* **1997**, *123*, 155–161.
[15] G. I. Panov, A. K. Uriarte, M. A. Rodkin, V. I. Sobolev, *Catal. Today* **1998**, *41*, 365–385.
[16] M. H. Groothaert, P. J. Smeets, B. F. Sels, P. A. Jacobs, R. A. Schoonheydt, *J. Am. Chem. Soc.* **2005**, *127*, 1394–1395.
[17] R. A. Himes, K. D. Karlin, *Proc. Natl. Acad. Sci. USA* **2009**, *106*, 18877–18878.
[18] F. Cavani, N. Ballarini, S. Luciani, *Top. Catal.* **2009**, *52*, 935–947.
[19] P. Kubánek, B. Wichterlová, Z. Sobalik, *J. Catal.* **2002**, *211*, 109–118.
[20] J. Pérez-Ramirez, G. Mul, F. Kapteijn, J. A. Moulijn, A. R. Overweg, A. Doménech, A. Ribera, I. W. C. E. Arends, *J. Catal.* **2002**, *207*, 113–126.
[21] I. Yuranov, D. A. Bulushev, A. Renken, L. Kiwi-Minsker, *J. Catal.* **2004**, *227*, 138–147.
[22] P. Ratnasamy, R. Kumar, *Catal. Today* **1991**, *9*, 327–419.
[23] S. Bordiga, R. Buzzoni, F. Geobaldo, C. Lamberti, E. Giamello, A. Zecchina, G. Leofanti, G. Petrini, G. Tozzola, G. Vlaic, *J. Catal.* **1996**, *158*, 486–501.
[24] J. Perez-Ramirez, J. C. Groen, A. Brückner, M. S. Kumar, N. M. Debbagh, U. Bentrup, L. A. Villaescusa, *J. Catal.* **2005**, *232*, 318–334.
[25] G. Berlier, G. Spoto, P. Fisicaro, S. Bordiga, A. Zecchina, E. Giamello, C. Lamberti, *J. Microchem.* **2002**, *71*, 101–116.
[26] A. A. Battiston J. H. Bitter, W. M. Heijboer, F. M. F. de Groot, D. C. Koningsberger, *J. Catal.* **2003**, *215*, 279–293.
[27] J. Jia, Q. Sun, B. Wen, L. X. Chen, W. M. H. Sachtler, *Catal. Lett.* **2002**, *82*, 7–11.
[28] A. A. Battiston, J. H. Bitter, D. C. Koningsberger, *J. Catal.* **2003**, *218*, 163–177.
[29] B. Ensing, F. Buda, P. E. Blöchl, E. J. Baerends, *Phys. Chem. Chem. Phys.* **2002**, *4*, 3619–3627.
[30] B. Ensing, F. Buda, M. C. M. Gribnau, E. J. Baerends, *J. Am. Chem. Soc.* **2004**, *126*, 4355–4365.
[31] A. Rosa, G. Ricciardi, E. J. Baerends, *Inorg. Chem.* **2010**, *49*, 3866–3880.
[32] K. E. Liu, C. C. Johnson, M. Newcomb, S. J. Lippard, *J. Am. Chem. Soc.* **1993**, *115*, 939–947.
[33] A. Bosnjakovic, S. Schlick, *J. Phys. Chem. B.* **2006**, *110*, 10720–10728.
[34] K. Yoshizawa, *J. Inorg. Biochem.* **2000**, *78*, 23–34.

